Understanding the influence of state/phase transitions on ice recrystallization in Atlantic salmon (*Salmo salar*) during frozen storage

Roopesh M. Syamaladevi[1], Kalehiwot N. Manahiloh[2], Balasingam Muhunthan[2] and Shyam S. Sablani[1]*

[1]*Biological Systems Engineering, Washington State University,*

P.O Box 646120, Pullman WA 99164-6120, USA

[2]*Civil and Environmental Engineering, Washington State University,*

PO Box 642910, Pullman WA 99164-2910

***Corresponding author**

Dr. Shyam S. Sablani

Biological Systems Engineering Department, Washington State University, P.O Box 646120, Pullman WA 99164-6120, USA

(Email: ssablani@wsu.edu; Tel: +509 335 7745; Fax: +509 335 2722)

Support: This activity was funded, in part, by a Biological and Organic Agriculture (BioAg) Program Grant from the Center for Sustaining Agriculture and Natural Resources at Washington State University

ABSTRACT

Temperature fluctuations during storage and distribution of frozen foods lead to ice recrystallization and micro-structural modifications that can affect food quality. Low temperature transitions may occur in frozen foods due to temperature fluctuations, resulting in less viscous and partially melted food matrices. This study systematically investigated the influence of state/phase transitions and temperature fluctuations on ice recrystallization during the frozen storage of salmon fillets. Using a modulated differential scanning calorimeter, we identified the characteristics glass transition temperature (T_g') of -27°C and the onset temperature for ice crystal melting (T_m') of -17°C in salmon. The temperature of salmon fillets in sealed plastic trays was lowered to -35°C in a freezer to achieve the glassy state. The temperature (T) of frozen salmon fillets in sealed plastic trays was modulated to achieve a rubbery state ($T>T_m'$), a partially-freeze-concentrated state ($T_g'<T< T_m'$), and a glassy state ($T<T_g'$). We performed temperature modulation experiments by exposing packaged salmon to room temperature twice a day for 2 to 26 minutes during four weeks of storage. We also analyzed ice crystal morphology using environmental Scanning Electron Microscopy (SEM) and *X*-ray Computed Tomography (CT) techniques to observe the pore distribution after sublimation of ice crystals. Melt-refreeze and isomass rounding mechanisms of ice recrystallization were noticed in the frozen salmon subjected to temperature modulations. Results show that ice crystal growth occurred even in the glassy state of frozen salmon during storage, with or without temperature fluctuations. Ice crystal size in frozen salmon was greater in the rubbery state ($T>T_m'$) due to the increased mobility of unfrozen water compared to the glassy state. The morphological/geometric parameters of ice crystals in frozen salmon stored for one month differed significantly from those in 0 days storage. These findings are important to the frozen food industry because they can help optimize

storage and distribution conditions and minimize quality loss of frozen salmon due to recrystallization.

Key words: Melt-refreeze, glass transitions, computer tomography, degree of anisotropy, ice crystal size, percent object volume, object surface/volume ratio

INTRODUCTION

Ice recrystallization causes textural changes that adversely affect frozen food quality during storage and distribution. Recrystallization is the process of increasing the size and shape of ice crystals and the rates of recrystallization depend on storage and distribution conditions[1]. Small ice crystals formed by quick freezing are thermodynamically unstable due to their high free energy[2]. They tend to grow on larger, more stable ice crystals during storage. The diffusion of unfrozen water depends on viscosity and temperature, and increases crystal growth at higher frozen storage temperatures[3]. Temperature fluctuations during storage and distribution are often unavoidable, aggravating the rate of recrystallization and other quality degradation reactions in frozen foods. Many mechanisms of recrystallization have been proposed; isomass recrystallization refers to the rounding of irregular shaped ice crystals to form compact ice crystals when the matrix achieves equilibrium as storage time increases[1]. The melt-refreeze recrystallization mechanism is commonly associated with foods stored at fluctuating temperatures (Figure 1). Temperature fluctuations may result in the partial melting and refreezing of ice, which further increases recrystallization rates. Partial melting due to increases in storage temperatures causes ice crystal size reduction. However, further cooling results in ice crystal growth and higher recrystallization rates (Figure 1)[1]. Ice recrystallization and temperature fluctuations during storage of ice cream, sugar solutions, and beef have been extensively studied, since they cause undesirable textural changes[4,5,6,7].

If the temperature of foods with high water content is lowered enough to restrict molecular motion, a freeze-concentrated glassy state characterized by high viscosity ($10^{12\text{-}14}$ Pas) occurs[8]. Many foods are quick-frozen to ensure small ice crystals and allow vitrification or amorphous glassy state formation using cryogenic freezing techniques. However, the advantages of quick-freezing may be annulled by temperature fluctuations, which may result in state transitions (e.g., glass transitions) and phase transitions (e.g., ice melting) when temperatures rise above characteristic glass transition (T_g') and onset of ice crystal melting (T_m') in frozen foods during the freeze-thaw cycle. Foods are expected to be most stable when stored in their high viscosity glassy state, which is attributed to low physicochemical degradation rates by restricted molecular motion. However, a transition from the glassy state to the less viscous rubbery state is observed at T_g'. Above T_m', the frozen matrix becomes less viscous as the amount of unfrozen water increases[8,9]. The rates of various diffusion-limited reactions are enhanced considerably above T_m' with an increase in molecular mobility. In frozen foods, T_g' and T_m' are of practical importance, since diffusion-controlled reaction rates in foods are greatly reduced below their T_g' [8,9]. Our research provides a better understanding of the influence of state/phase transitions due to temperature fluctuations on diffusion-controlled changes such as ice recrystallization. The results of this research can help the food industry optimize storage and distribution conditions and minimize quality loss due to recrystallization.

Environmental Scanning Electron Microscopy (SEM) and *X*-ray Computed Tomography (CT) techniques have been used to analyze ice crystal shape, size, and distribution in frozen foods[1,10,11]. *X*-ray CT is relatively a new technique in food research, and has been used to characterize pore size, microstructure, crispness, and ice crystal sization[10,11]. It gives superior advantages to non-destructively observe the internal three-dimensional (3D) structures of foods

without extensive sample preparation. This technique eliminates the disadvantages of microstructural disturbances during cutting and sample preparation that may occur with other methods (e.g. SEM)[10]. The objective of the current study was to understand the influence of glass transitions and temperature fluctuations on ice recrystallization during the freeze-thaw cycle of Atlantic salmon fillet (*Salmo salar*) using an environmental scanning electron microscope and *X*-ray CT.

MATERIALS AND METHODS

Fresh salmon fish (*Salmo salar*) was purchased from a local grocery store. The thermal transitions of salmon were determined using differential scanning calorimetry (DSC, Q2000, TA Instruments, New Castle, DE)[12,13]. The calorimeter was calibrated for temperatures and enthalpies of fusion using indium and sapphire. A mechanical refrigerated cooling system was used to cool the samples inside DSC. An empty, sealed aluminum pan was used as a reference in each test. A small quantity (10–20 mg) of fresh salmon was hermetically sealed inside in aluminum pans (volume 30 µL) and cooled from room temperature to -90°C at 5°C/min and equilibrated for 10 min. After equilibration, salmon samples were heated from -90°C to 70°C at a rate of 5°C/min. TA Instruments Universal analysis software was used to analyze DSC thermograms. For fresh salmon, thermograms provided the melting endotherm, and the T_m' was identified as the intersection point of the baseline with the left side of endotherm (Figure 2). Later, annealing experiments were conducted at (T_m'-1) for 30 minutes and the samples were scanned from (T_m'-1) to -90°C at 5°C/min. To identify the glass transition temperature (T_g'), the salmon samples were heated from -90°C to 70°C at 5°C/min. The T_g' was identified as a vertical shift in the heat flow curve of DSC thermogram (Figure 2). The T_g' and T_m' of salmon were identified using DSC as -27 and -17°C, respectively.

116 The protocol for recrystallization experiments is presented in Figure 3. Initially, fresh salmon
117 was cut into rectangular pieces (12.5 cm×9 cm×2.5 cm) and sealed into rectangular plastic trays
118 (15.2 cm×11.5 cm×3.3 cm). Salmon samples were frozen at -35°C to achieve a glassy state. The
119 temperature of salmon (T) was modulated 5°C above T_m' to achieve a rubbery state, 5°C above
120 T_g' or 5°C below T_m' to achieve a partially freeze-concentrate state, and 5°C below T_g' by
121 exposing the salmon samples to room temperatures (23°C) for a predetermined time. The times
122 required to reach the state/phase transition temperatures from the storage temperature (-35°C)
123 were determined by monitoring the surface and center temperatures of the frozen salmon using
124 an LTC thermocouple temperature data logger with an internal and external *K*-type thermocouple
125 (Supco LOGiT series data loggers, Allenwood, NJ). The required times to reach the state/phase
126 transition temperatures (-12, -22, and -32°C) from -35°C were 26, 12 and 2 min, respectively.
127 The surface and center temperatures of the salmon during 1 month of frozen storage were
128 monitored. Temperature fluctuation experiments were conducted twice a day (every 12 hours)
129 for one month. A control salmon sample without any temperature modulation was also stored at -
130 35°C for one month.

131 The ice crystal size in freeze-dried salmon samples was analyzed every week, which is an
132 indirect method of determining ice crystal size distribution in frozen foods[14,15]. The pore size
133 distribution of freeze-dried products is assumed to represent ice crystal size distribution in frozen
134 products. Each week, the frozen salmon samples were taken out from the freezer and kept inside
135 a freeze-dryer (Virtis freeze mobile 24 with Unitop 600 L, VirTis SP Industries Co., New York).
136 Initially, the shelf temperature, condenser temperature and vacuum inside the freeze dryer shelf
137 were set to -20, -60°C and 20 Pa, respectively. To avoid ice melting and structural collapse in
138 salmon, the freeze drying chamber temperature was set at 5°C for the first two days and

increased to 20°C later[14,15]. After 72 hours of freeze drying, the salmon pieces were removed and stored in Ziploc bags at -20°C until further analysis.

Scanning Electron Microscopy (SEM): The freeze-dried samples were cut into 2-3 mm slices with a stainless steel razor perpendicular to the direction of heat flux, and analyzed using an environmental scanning electron microscope (SEM) (FEI Co. [Field Emission Instruments], Hillsboro, OR) with magnifications from 100 to 250 times. The surface and center temperature of the salmon slices were monitored during storage. Since the location of the slices selected may influence the ice crystal size distribution, at least 2 to 3 slices from different parts (center and near the surface) of each sample were taken randomly for pore size analysis. Micrographs of the freeze-dried salmon were analyzed for pore size distribution of 200 pores using a Leica image analysis system (Leica Microsystems Inc. Buffalo Grove, IL, USA). The equivalent pore diameter was determined using minor and major axes (major diameter × minor diameter)$^{0.5}$ [16]. The median ice crystal size (X_{50}) was determined as the equivalent ice crystal diameter corresponding to 50% of the cumulative distribution function of the sample[1]. The ice crystal size distribution in frozen salmon subjected to temperature modulation was characterized by X_{50}, the slope of the cumulative distribution at $X_{50,}$ and the percentage ice crystal growth rate[17]. The percentage ice crystal growth rate and the slope were determined with Equations 1 and 2, respectively.

$$\% \text{ ice crystal growth rate} = \frac{\left(\text{Final } X_{50} - \text{Initial } X_{50}\right)}{\text{Initial } X_{50}} \quad (1)$$

$$\text{Slope} = \frac{0.5}{X_{50}} \quad (2)$$

159 X_{50} better represents the ice crystal size population than the arithmetic mean, since it evaluates
160 the central tendency better especially for a skewed data set[1]. Normally, median values of ice
161 crystal size are smaller than mean values when the number of smaller ice crystals is greater than
162 that of large ice crystals[1].
163 *X-ray Computer Tomography* (*CT*): In this study, we examined and evaluated selected pore
164 parameters of salmon from images obtained with *X*-ray Computed Tomography scanning (CT
165 scan). We calculated the geometric properties of horizontal two-dimensional (2D) image slices
166 integrated over the height of samples in order to visualize 3D properties. The Washington State
167 High-resolution X-ray Computed Tomography (WAX-CT) hosts *X*-ray CT scan system (HYTEC
168 Sensors & Imaging Group, Inc. (HYSIG), Los Alamos, NM) with two *X*-ray sources that are
169 capable of generating a 420 keV and 225 keV. The 420 keV source is preferably used for
170 relatively bigger samples where adequate detail of sample constituent structures can be
171 visualized with a relatively lower resolution. The 225 keV source generates *X*-ray beams at a
172 lower energy as compared to those from the 420 keV and is suited for smaller samples involving
173 very fine details as the *X*-ray beams are micro focused. These two *X*-ray sources are networked
174 to a central work station, a processing platform that consists of four parallel computing
175 processors each equipped with double core CPUs and set of software that control the scanning
176 process and subsequent image analyses. This study used the 225 keV micro-focused source to
177 achieve enhanced resolution[18,19]. The CT scanning involved several steps: placing the specimen
178 on the rotary stage, initiating the data acquisition from the work station, recording *X*-ray
179 intensities before and after penetrating the specimen while rotating the specimen at small angles,
180 collecting CT numbers over a full revolution, and analyzing CT numbers[19] to return sinograms of
181 each slice.

In this study, 150 keV and 164 μA energy-flux combination gave sufficient resolution to allow clear identification of fibers and void spaces. The detector used was a Varian PaxScan 2520 with CsI Scintillator in fast-scan, 2x2 binning mode and a frame rate of 7.5 frames per second. The detector was fully calibrated to gather 200 frames for both dark and gain-field capturing. The initiation and sinogram generation was handled with FlashCT DAQ, the first of the three software packages synchronized with the Flat panel Amorphous Silicon High-resolution Computed Tomography (FlashCT) *X*-ray system. After scanning, we reconstructed the 2D slices with the FlashCT DPS software. In this stage, any centering flaw in the scanning phase could be corrected by adjusting the slope and intercept of the sinograms, referred to as image-centering correction. This was a very useful capability of the FlashCT DPS software that prevents a resolution reduction of up to 50% from one pixel of misalignment[19]. After successful generation of 2D slices, we used FlashCT VIZ software to assemble the reconstructed slices into a 3D virtual representation of the specimens. We then transferred the images to post-image processing software called Image-Pro-Plus. In order to carry out such tasks, we developed and ran macros on the Image-Pro-Plus platform to post-process and quantify the following geometric parameters[11]:

a. Percent object volume (POV) to determine the proportion of the volume of pores in freeze-dried salmon or the volume of ice crystals in frozen salmon.
b. Object surface/volume ratio (OSVR) to characterize the size and distribution of pores in salmon.
c. Degree of anisotropy (DA) to characterize the alignment of pores, indicating the 3D structural symmetry of freeze-dried salmon..

d. Median ice crystal size (X_{50}) to characterize the size of pores or ice crystal diameter in frozen salmon.

The degree of anisotropy is a measure that indicates the presence or absence of preferential alignment of structures along a specific direction (Lim and Barigou, 2004). DA is usually calculated using mean intercept length and Eigen vector analysis. This is done drawing a fan of lines through the test volume over the full range of 3D angles. In addition, for each angle several parallel lines are drawn covering the entire test volume and the mean intercept length for that angle is calculated as an average of these lines. If the object is isotropic, the lines traversing it at any angle will pass through a similar length of pore phase as a proportion of its total length. Based on an Eigen vector analysis of the mean lengths the degree of anisotropy (DA) is obtained[20] as:

$$DA = 1 - \frac{\min eigenvalue}{\max eigenvalue} \quad (3)$$

A value of 0 would correspond to isotropy whereas a value of 1 would indicate total anisotropy. During post-processing, images were converted t_o an 8-bit file format to reduce memory consumption. In the next step of image segmentation, salmon samples were presumed to be dominated by two phases such as solid and void, and segmentation was applied accordingly. We input image-processing algorithms with threshold values to analyze the images and return values for the desired geometric properties.

Salmon ice crystals/pores data were analyzed for statistical significance using SAS 9.1 (SAS Institute, Inc., Cary, NC, USA). A value of $P < 0.05$ was selected as statistically significant using the Two-Way ANOVA by Least Square Difference (LSD) method.

RESULTS AND DISCUSSION

226 We conducted an indirect characterization of ice crystals in frozen salmon by analyzing the pores
227 in freeze-dried salmon. We interpreted SEM micrographs to determine the median ice crystal
228 size $X_{(50)SEM}$ (μm) in frozen salmon. Freeze-dried salmon exhibited fiber networks and holes
229 representing ice crystals, as shown in SEM micrographs (Figures 4, 5). SEM micrographs
230 indicated that ice crystals were small and irregular in frozen salmon immediately after freezing
231 (Figures 4, 5). Networks of ice crystals formed with increasing storage time, probably due to the
232 diffusion of unfrozen water (Figures 4, 5). Ice crystals became more spherical and regular in
233 shape during storage (Figures 4, 5). Melt-refreeze and isomass rounding are the proposed
234 mechanisms of recrystallization in frozen salmon subjected to freeze-thaw cycles. In commercial
235 frozen foods, the melt-refreeze recrystallization mechanism is the most common type of
236 recrystallization[1].

237 We used *X*-ray CT images to characterize ice crystal distribution in salmon by analyzing more
238 than 200 images. The *X*-ray tomography images (Figures 6, 7) differed significantly from the
239 SEM images[21]. Fiber-entangled networks and pores left by ice crystals were clearly visible in the
240 orthogonal slices in three dimensions (X, Y, and Z axes) of *X*-ray tomography images (Figures 6,
241 7), while SEM micrographs provided only two-dimensional representation of the microstructure
242 of freeze-dried salmon. As evident in the *X*-ray tomography images, the direction of ice crystals
243 appears to form in the direction of the fibers (Figures 6, 7). This demonstrates the influence of
244 food microstructure on ice crystal shape during freezing and frozen storage[21]. From the scanned
245 CT images we determined selected geometric parameters, including percent object volume
246 (POV) (%); object surface/volume ratio (OSVR) (1/μm), degree of anisotropy (DA) and average
247 diameter (μm), that characterize the pores in freeze-dried salmon. The median values of POV,
248 OSVR, and the average diameter are presented[1].

249 The $X_{(50)CT}$ values were greater than the $X_{(50)SEM}$ values obtained for similar experimental
250 conditions (Table 1, 2 and Figures 8-10). This difference in the X_{50} values is attributed to the
251 differences in the principles and methods of determination. We determined the equivalent
252 diameter of the pores with SEM, using major and minor diameters of the pores. We determined
253 the average diameter of pores with tomography by equating pore volume to sphere volume. We
254 obtained the $X_{(50)CT}$ from 3D pore size distribution and the $X_{(50)SEM}$ values from SEM and 2D
255 pore-size distribution. With SEM, the location of the slices selected for analysis may also
256 influence the ice crystal size distribution, since relatively larger ice crystals were observed near
257 the surface of frozen foods (due to temperature fluctuations) as compared to the center. However,
258 for frozen salmon, the monitored center and surface temperatures were relatively similar during
259 storage (data not shown). In *X*-ray CT, location of the ice crystals may not influence their size
260 distribution, since the ice crystal size is averaged over a number of slices. The $X_{(50)CT}$ of frozen
261 salmon (~659 µm) in our study (Table 2) is comparable to the average ice crystal size values
262 (~500 µm) of boneless frozen pink salmon fillet using *X*-ray CT, as reported by Mousavi et al.[21].

263 We identified a significant interaction between state/phase transitions of frozen salmon and
264 storage time on ice recrystallization with two-way statistical analysis using the SAS program.
265 The effects of storage time and state transition on recrystallization are presented in the following
266 sections.

267 **Effect of storage time on ice recrystallization**

268 Our study found that, in general, ice crystal size increases and the number of ice crystals
269 decreases in salmon during frozen storage due to recrystallization, irrespective of state/phase
270 transitions (Table 1 and Figures 4, 5). The $X_{(50)SEM}$ and $X_{(50)CT}$ of frozen salmon after four weeks
271 of storage were significantly greater than the initial $X_{(50)}$ values. For instance, the initial $X_{(50)SEM}$

was 121.4 μm in frozen salmon, while the $X_{(50)SEM}$ ranged between 148.3-221.4 μm after storage, depending on state/phase transitions (Table 1). Similarly, the initial $X_{(50)CT}$ was 658.6 μm, while the $X_{(50)CT}$ ranged between 1105-1644.1 μm after storage, depending on state/phase transitions. A broadening of ice crystal size distribution and a decrease in slope in the cumulative distribution of equivalent ice crystal diameter indicated an increase in the roundness of ice crystals. This suggests that the ice crystals became more spherical with time (Figures 4, 5). This change in shape of ice crystals may be attributed to the increase in diffusion of unfrozen water during storage; a strong correlation between the diffusion coefficient of water and recrystallization rate in frozen foods has been reported in previous research[22].

Our study found that the mean POV values of ice crystals in frozen salmon after four weeks of storage with or without state/phase transitions (56.5-64.4) was significantly greater than the initial mean POV value (49) (Figure 10 and Table 2). The increase in POV indicates the increase in the volume of pores in freeze-dried salmon or ice volume in frozen salmon due to recrystallization. This increase in POV can be attributed to the conversion of unfrozen water to ice in frozen salmon during storage. Previous research suggests that frozen foods prepared by quick-freezing techniques may contain some amount of unfrozen water, even at low temperatures. However, this unfrozen water in foods may eventually convert to ice attributed to various structural relaxations over the time.

Our study found that the initial OSVR value (3.33) of ice crystals in salmon immediately after freezing was significantly greater than the OSVR values (0.57-0.64) of ice crystals in salmon after four weeks (Figure 10). OSVR is related to the shape of the ice crystals. A decrease in OSVR may indicate a decrease in surface area, an increase in volume, or both. Results show that during recrystallization, a decrease in the number of ice crystals and an increase in the size of ice

crystals occur. Also, the ice crystals become more spherical in nature resulting in their reduced surface area during storage. This decrease in surface area and the increase in POV contributed to the decrease in OSVR during storage. The degree of anisotropy (DA) characterizes the symmetry, indicating the alignment of ice crystals in frozen salmon. The DA value of ice crystals obtained for salmon immediately after freezing (0.97) was close to 1, the ice crystals are anisotropic in nature (Table 2), showing high variation in the pattern of void spaces. A decrease in DA (from 0.97 to 0.83) of ice crystals in frozen salmon indicates that the ice crystals became regular in shape and symmetrical in nature with time.

Effect of state transitions on ice recrystallization

This study found that the mean ice crystal size change in frozen salmon during storage was dependent on the types of transitions (e.g., glass-to-partial-freeze-concentrated or glass-to-rubber transitions), regardless of the time of storage (Table 1 and Figures 8-11)[4]. We observed an increase in $X_{50(\mathrm{SEM})}$, $X_{(50)\mathrm{CT}}$ and a broadening of ice crystal size distribution. This was characterized by a decrease in slope in the cumulative distribution of equivalent ice crystal diameter according to the type of transition (glass-to-partial-freeze-concentrated and glass-to-rubber transition) in the frozen salmon samples (Figures 8-11). The ice crystals became more spherical in nature (Figures 4, 5) and the POV, OSVR and DA values of ice crystals in frozen salmon varied, depending on the nature of state transitions. (Figures 10 and 11). Specific changes in the selected structural parameters of ice crystals in frozen salmon due to state/phase transitions are described in following sections.

Glassy state storage without temperature modulations: In this study, we observed ice crystal growth even in the glassy state ($<T_g'$). The $X_{(50)\mathrm{SEM}}$ of ice crystals in frozen salmon increased from 121.4 to 148.3 μm (22.1% growth in ice crystal size) during one month of storage at -35°C

318 (Figures 8-10). Ice crystal distribution broadened with time, indicated by a decrease in slope in
319 the cumulative distribution of equivalent ice crystal diameter from 0.412 to 0.337. This also
320 indicates an increase in ice crystal size (Table 1). The $X_{(50)CT}$ of ice crystals in frozen salmon
321 increased from 659 to 1105 μm (68 % growth in ice crystal size) in the glassy state. This
322 indicates that the rates of diffusion-limited reactions, such as recrystallization, do not completely
323 cease in the glassy state. As noted earlier, structural relaxations may occur in frozen foods in the
324 glassy state, resulting in molecular rearrangements and the diffusion of unfrozen water[22].

325 Our study found a significant increase (from 49 to 57) in the POV of ice crystals in frozen
326 salmon in the glassy state as compared to the initial POV (Figure 10 and Table 2). As stated
327 earlier, the increase in POV, represented by an increase in the size and proportion of ice crystals,
328 is attributed to the conversion of unfrozen water to ice in frozen salmon during storage. The
329 OSVR of ice crystals in frozen salmon decreased (3.33 to 0.64) in frozen salmon in the glassy
330 state compared to the initial OSVR (Table 2 and Figure 10). This indicates that the ice crystal
331 size distribution became broader and the ice crystals became more spherical in frozen salmon
332 during storage. A small decrease in DA (0.97 to 0.96) showing the ice crystals became more
333 regular (Table 2).

334 Carrington et al.[23] stored 30% fructose solution at -75°C for two weeks far below its T_g' (-
335 58°C) and observed ice recrystallization. Hagiwara et al.[22] reported an increase in mean ice
336 crystal radius of sucrose solution during 20 hours of storage at -50°C (the glassy state).
337 Kontogiorgos and Goff[24] reported an increase in ice crystal size in frozen hydrated gluten during
338 one month of storage in the glassy state (-13°C). Thermodynamically, glassy systems are not at
339 equilibrium, and structural relaxations/rearrangements may occur below glass transition
340 temperature[22]. During freezing/low temperature storage, a large quantity of unfrozen water is

341 vitrified, depending on how far the freezing/storage temperature goes below T_g'. The quantity of
342 unfrozen water present may be enough for recrystallization to occur by diffusion, even with
343 limited molecular motion (rotational and vibrational molecular motion) as shown by structural
344 relaxation at low temperatures[22,23]. More research is needed to further understand the relationship
345 between structural relaxation and molecular mobility, as the rate of ice recrystallization may be
346 related to enthalpy/structural relaxations and the physical stability of frozen systems in their
347 glassy states.

348 *Glassy-state storage with temperature modulations*: In our study, when frozen salmon was
349 exposed to room temperature (23°C) for two minutes, the temperature of the salmon increased
350 from -35 to -32°C; however, the sample was below its T_g'. The $X_{(50)SEM}$ increased significantly
351 from 121.4 to 176.4 (45.3% growth in ice crystal size) in frozen salmon in the glassy state
352 (Figures 8, 9 and Table 1). The $X_{(50)CT}$ of frozen salmon without any state transitions increased
353 from an initial $X_{(50)CT}$ of 659 to 1090 μm (65% growth in ice crystal size) after one month (Table
354 2). The $X_{(50)SEM}$, $X_{(50)CT}$, POV, OSVR and DA values of frozen salmon in glassy state with
355 temperature modulation indicate that the size of ice crystals remained comparable. However,
356 they became more regular and spherical in shape as compared to the frozen salmon that did not
357 undergo any temperature fluctuation during storage.

358 *Glass-to partial-freeze-concentrated transitions*: Our study found that when frozen salmon was
359 exposed to room temperature (23°C) for 12 minutes, the temperature increased from -35 to -
360 22°C, which lies between its T_g' and T_m'. The glass-to-partial-freeze-concentrated transition
361 during storage increased $X_{(50)SEM}$ from 121.4 to 184.9 μm (52.3% growth in ice crystal size). The
362 percentage growth rates of ice crystals in glassy and partially-freeze-concentrated salmon
363 matrices were 45.3 and 52.3% respectively. Computed tomography analysis showed increase of

364 $X_{(50)CT}$ from 659 to 1540 μm (134% growth in ice crystal size). The greater percentage of ice
365 crystal size growth in partial-freeze-concentrated salmon compared with that of glassy salmon
366 may be attributed to the increased molecular mobility and diffusion of unfrozen water[1]. Previous
367 studies have confirmed a strong correlation between the diffusion coefficient of water and the
368 recrystallization rate in frozen foods[22].

369 The OSVR values of ice crystals in the partially-freeze-concentrated salmon matrix during
370 one month of storage were comparable to the OSVR of ice crystals in glassy salmon, indicating
371 that partial melting and refreezing of ice crystals did not contribute to the modification of the
372 shape of ice crystals. When frozen foods are subjected to phase/state transitions, melting and
373 disappearance of smaller ice crystals may occur due to their higher melting point, surface area
374 and free energy[1].

375 *Glass-to-rubber transitions*: Our study found that a more regular pore/ice crystal shape was
376 achieved when the glass-to-rubber transition occurred in frozen salmon during storage (Figure
377 9). The $X_{(50)SEM}$ increased from 121.4 to 221.4 μm (82.4% growth in ice crystal size) in salmon
378 at the rubbery state (Figures 8). The $X_{(50)CT}$ increased from 659 to 1644 μm (149% growth in ice
379 crystal size). The ice crystal size growth in salmon in the rubbery state may be attributed to the
380 melting and refreezing of ice. Our results show that in the rubbery state, an increase (from 49 to
381 64) in POV of ice crystals occurs in salmon as compared to the initial POV (Figure 10 and Table
382 2). This significant increase (p value < 0.05) in POV after the glass-to-rubber transition in frozen
383 salmon may be attributed to the increased molecular mobility of unfrozen water in the rubbery
384 state, aggravating the unfrozen water to ice conversion. However, this study found that the POV
385 and OSVR of ice crystals in frozen salmon with the glass-to-rubber transition were not

significantly different (p value ≥ 0.05) from the frozen salmon with the glass-to-partial-freeze-concentrated transition (Figure 10 and Table 2).

DISCUSSION

The enhancement of recrystallization rates by glass-to-rubber state transition in frozen salmon can be attributed to an increase in molecular mobility. This is probably due to the increased kinetic energy and reduced viscosity of the matrix through ice melting and an increase in the amount of unfrozen water[9,25]. Mobility of unfrozen water in the freeze concentrated matrix is considered to be one of the main factors affecting recrystallization rate. Hagiwara et al.[22] reported that the self-diffusion coefficient of water molecules and the recrystallization rate in freeze-concentrated sugar solutions are positively correlated; however, the diffusion of solute particles may not contribute much to recrystallization as compared to water diffusion. The diffusion of unfrozen water from small to large ice crystals is aggravated by temperature fluctuations and state transitions, resulting in an increase in translational and rotational mobility of water and solute molecules[22,26].

Ablett et al.[26] observed a good correlation between the recrystallization rate and (T-T_g') in the rubbery state of frozen carbohydrate matrices, highlighting the importance of T_g';. They also reported a strong correlation between water and solute mobility and T_g'. Carrington et al.[23] stored 30% fructose solution above T_g' (-58°C) at -25°C for two weeks, and observed a significant increase in the ice crystallization rate. This increase in translational mobility resulted in the diffusion of unfrozen water during devitrification and storage of a 30% fructose solution at -25°C[23]. Also, considerable recrystallization and an increase in ice crystal size by 20 or 30 times was observed in the rubbery state of 30% fructose solution as compared to the glassy state at -75°C for two weeks[23].

409 The values of morphological/geometric parameters of ice crystals in frozen salmon with
410 state/phase transitions differed significantly from those of frozen salmon without state/phase
411 transitions, indicating the importance of T_g' and T_m' in the recrystallization process. The ice
412 crystal size parameters of frozen salmon in the rubbery state were significantly higher than that
413 of partially-freeze-concentrated salmon, indicating that T_m' is an important temperature for the
414 ice crystal growth during storage. However, ice crystal shape-related parameters such as POV,
415 OSVR and DA in the rubbery state did not differ significantly from those of partially-freeze-
416 concentrated salmon, suggesting that T_g' is an important temperature for the shape of ice crystals.
417 The change in the size and shape of ice crystals contributes to the mechanical damage of tissues
418 due to ice crystal growth in frozen foods. Hence, the values of T_g' and T_m' should be considered
419 when designing appropriate frozen storage and distribution techniques, in order to avoid textural
420 degradation due to ice crystal growth.

421 *Kinetic model for ice recrystallization in frozen salmon:* Previous research has proposed many
422 kinetic models, based on the theoretical considerations of the Ostwald ripening principle of ice
423 recrystallization in frozen foods. In our study, the recrystallization process in frozen salmon can
424 be described as[4,27]:

425 $$(D - D_o) = A + k\, t^{\frac{1}{n}} \quad (4)$$

426 where D is the mean ice crystal size after time t, D_o is the initial mean ice crystal size, k is the
427 recrystallization rate constant, A is a constant, and n is the power-law exponent. Our research
428 data for frozen salmon was fitted to Equation 4 with different n values. A value for n = 3 was
429 selected based on the highest R^2 value when fitted with recrystallization data. An increase in (D-
430 D_o) was observed, with $t^{0.33}$ for the frozen salmon with state transitions during storage (Figure

12). However, a significant increase in the slope of (D-D_o) Vs $t^{0.33}$ curve for frozen salmon with glass-to-rubber transition was observed in comparison to the ice crystal size of frozen salmon without any state transition (below T_g') and with glass-to-partial-freeze-concentrated transition (between T_m' and T_g') (Figure 12). The recrystallization rate constants (k) obtained for frozen salmon subjected to temperature modulations from -35°C to -32 (glassy state), -22 (glass-to-partial-freeze-concentrated transition), and -12°C (glass-to-rubber transition) by fitting the recrystallization data with Equation 3 were 35.8, 40.7, and 61.5 week^{-1}, respectively (Figure 13).

To elucidate the relationship between recrystallization rate and glass transitions, the recrystallization rate constants (k) for frozen salmon with state transitions were found to be related to the extent of temperature modulation from the T_g' i.e. (T-T_g') (Figure 13). As the value of (T-T_g') increased, a non-proportional increase in the value of k was observed for frozen salmon, and this is attributed to state/phase transitions. A dramatic increase in the value of k for frozen salmon with glass-to-rubber transitions occurred, as indicated by an obvious change in slope. This demonstrates the importance of T_g' and T_m' in preserving the quality of frozen foods during storage. Temperature fluctuations are often unavoidable, however, it is essential to keep the product temperature below T_g' and T_m' to avoid the texture degradation due to ice crystal growth during storage and distribution.

CONCLUSIONS

Our study found that ice crystal size, broadness of ice crystal size distribution, and roundness increase while the number of ice crystals decreases in frozen salmon, depending on the types of transitions and storage time. Significant ice crystal growth in the glassy state of frozen salmon indicates that continued molecular mobility occurs in the thermodynamically unstable glassy state. We found that the degree of anisotropy (DA) of ice crystals decreases during storage, as ice

crystals became more regular in shape. However, DA values were close to 1, indicating that the alignment of ice crystals is greatly anisotropic in nature. Results show that the proportion of ice crystals in frozen salmon increases due to recrystallization, indicated by an increase in percent object volume (POV). Results also show that ice crystals became more spherical, as indicated by a decrease in object surface/volume ratio (OSVR). The significant increase in the recrystallization rate constant in frozen salmon subjected to temperature modulations above T_m' and T_g' demonstrates the importance of these temperatures to avoid quality degradation in frozen foods during storage.

ACKNOWLEDGEMENTS

This activity was funded, in part, by a Biological and Organic Agriculture (BioAg) Program Grant from the Center for Sustaining Agriculture and Natural Resources at Washington State University. Technical helps from Dr. Valerie Lynch-Holm, Franceschi Microscopy and Imaging Center, and Frank Younce, Pilot plant, WSU are acknowledged.

REFERENCES

1. A.A. Flores, H.D. Goff, J. Dairy Sci. **82(7)**, 1408-1415 (1999)
2. R. L. Sutton, A. Lips, G. Piccirillo, J. Food Sci. **61(4)**, 741-745 (1996)
3. S. Adapa, K.A. Schmidt, I.J. Jeon, T.J. Herald, R.A. Flores, Food Rev. Int. **16(3)**, 259-271 (2000)
4. D.P. Donhowe, R.W. Hartel, Int. Dairy J. **6**, 1191-1208 (1996a).
5. A. Regand, H. D. Goff, J. Dairy Sci. **85(11)**, 95-102 (2002).
6. T. Hagiwara, R.W. Hartel, S. Matsukawa, Food BioPhy. **1(2)**, 74-82 (2006).
7. M. N. Martino, N. E. Zaritzky, J. Food Sci. **53(6)**, 1631-1637 (1988).

476 8. H.D. Goff, M.E. Sahagian, Thermochim. Acta. **280**, 449-464 (1996).
477 9. S.S. Sablani, R.M. Syamaladevi, B.G. Swanson, Food Eng. Rev. **2**, 168-203 (2010)
478 10. R. Mousavi, T. Miri, P. W. Cox, P. J. Fryer, J. Food Sci. **70(7)**, E437-E442 (2005).
479 11. P. Frisullo, R. Marino, J. Laverse, M. Albenzio, M. A. Del Nobile, Meat Sci. **85**, 250-255
480 (2010).
481 12. R. M. Syamaladevi, S. S. Sablani, J. Tang, J. R. Powers, B. G. Swanson. J. Food Eng. **91**,
482 460-467 (2009).
483 13. R. M. Syamaladevi, S. S. Sablani, J. Tang, J. R. Powers, B. G. Swanson. Thermochim. Acta
484 **503-504**, 90-96 (2010).
485 14. D. Chevalier, A. Le Bail, M. Ghoul, J. Food Eng. 46(4), 277-285 (2000)
486 15. B. Woinet, J. Andrieu, M. Laurent, S.G. Min, J. Food Eng. **35(4)**, 395-407 (1998).
487 16. O. Miyawaki, T. Fujii, Y. Shimiya, Food Sci. Technol. Res. **10(4)**, 437-441 (2004).
488 17. A.P. Whelan, A. Regand, C. Vega, J.P. Kerry, H.D. Goff, Int. J. Food Sci. Technol. **43**, 510-
489 516 (2008).
490 18. P. Iassonov, T. Gebrenegus, M. Tuller, Water Res. Resear. **45**, (2009).
491 19. M. R. Razavi, B. Muhunthan, Al Hattamleh, GeoTech. Test. J. **30(3)**, 212-219 (2006).
492 20. K.S. Lim, M. Barigou, Food Res. Int. **37,** 1001-1012 (2004)**.**
493 21. R. Mousavi, T. Miri, P. W. Cox, P. J. Fryer, Int. J. Food Sci. Technol. **42**, 714-727 (2007).
494 22. T. Hagiwara, J. Mao, T. Suzuki, R. Takai, Food Sci. Technol. Res. **11(4)**, 407-411 (2005).
495 23. A.K. Carrington, H.D. Goff, D.W. Stanley, Food Res. Int. **29(2)**, 207-213 (1996)
496 24. V. Kongtogiorgos, H. D. Goff, Food Biophys. **1(4)**, 202-215 (2006).
497 25. T. Miller-Livney, R. W. Hartel, J. Dairy Sci. **80(3)**, 447-456 (1997).
498 26. S. Ablett, C.J. Clarke, M.J. Izzard, D.R. Martin, J. Sci. Food Agric. **82**, 1855-1859 (2002)

499 27. D. P. Donhowe, R.W. Hartel, Int. Dairy J. **6**, 1209-1221 (1996b).

500

Table 1. Mean ice crystal size, slope and % growth of ice crystal size during frozen storage of salmon with/without state transitions obtained from SEM micrographs

Storage time (days)	Time of temperature fluctuation											
	No temperature fluctuation ($T < T_g'$; glassy state)			($T < T_g'$; glassy state)			($T_g' < T < T_m'$; glassy to partial-freeze-concentrated state transition)			($T > T_m'$; glassy to rubbery state transition)		
	X_{50} (μm)	Slope	% ice crystal growth rate	X_{50} (μm)	Slope	% ice crystal growth rate	X_{50} (μm)	Slope	% ice crystal growth rate	X_{50} (μm)	Slope	% ice crystal growth rate
0	121.4	0.412	0	121.4	0.412	0	121.4	0.412	0	121.4	0.412	0
7	NA	NA	NA	143.7	0.348	18.4	180.6	0.277	48.8	172.8	0.289	42.3
14	NA	NA	NA	126.4	0.396	4.11	177.6	0.282	46.3	205.7	0.243	69.4
21	NA	NA	NA	174.8	0.286	43.9	181.2	0.276	49.2	200.9	0.249	65.5
28	148.3	0.337	22.1	176.4	0.283	45.3	184.9	0.27	52.3	221.4	0.226	82.4

Table 2. Selected geometric parameters of frozen salmon determined using *X*-ray CT

	Storage time				
	0 days	28 days			
	-	No temperature fluctuation ($T < T_g'$; glassy state)	($T < T_g'$; glassy state)	($T_g' < T < T_m'$; glassy to partial-freeze-concentrated state transition)	($T > T_m'$; glassy to rubbery state transition)
Median Ice Crystal Size (X_{50}) (μm)	658.6±134.7	1105±194.7	1090.7±188.4	1540.9±239.6	1644.1±264.2
Median Percent Object Volume, POV (%)	49±4.1	56.5±3.7	62.7±5.2	64±2.54	64.4±3.3
Median Object Surface/Volume Ratio, OSVR (1/μm)	3.33±0.4	0.64±0.05	0.61±0.04	0.57±0.04	0.62±0.04
Degree of Anisotropy (DA)	0.97	0.96	0.83	0.84	0.91

LGENDS TO FIGURES

Figure 1 Microscopic illustration describing the typical melt-refreeze recrystallization mechanism in a frozen food due to temperature fluctuations during storage and distribution. Temperature fluctuations result in warming and cooling cycles during storage. A). Frozen matrix with temperature T, immediately after freezing. B). Frozen food temperature goes from T to $T+\Delta T$ during warming cycle. Partial/complete melting of ice crystals and diffusion of water molecules may result in during warming. % ice content decreases and %unfrozen water content increases during warming cycle. C). Frozen food temperature goes from $T+\Delta T$ to T during warming cycle Refreezing during cooling results in growth on existing ice crystals. D). After storage, an increase in the average ice crystal size and decrease in the total number of ice crystals are observed with melt-refreeze recrystallization. Ice crystals become more regular and spherical in shape due to recrystallization.

Figure 2 Identification of T_g' and T_m' of frozen salmon using DSC thermograms

Figure 3 Protocol used for ice recrystallization experiment in frozen salmon during storage

Figure 4 Environmental scanning electron microscopy micrographs of freeze-dried salmon. Before freeze drying, frozen salmon was subjected state transitions during 4 weeks storage. (A): Immediately after freezing, (B): ($T < T_g'$), (C): ($T_g' < T < T_m'$), (D): ($T > T_m'$).

Figure 5 Environmental scanning electron microscopy micrographs of freeze-dried salmon. Before freeze drying, frozen salmon was subjected to glass-to-rubber transition

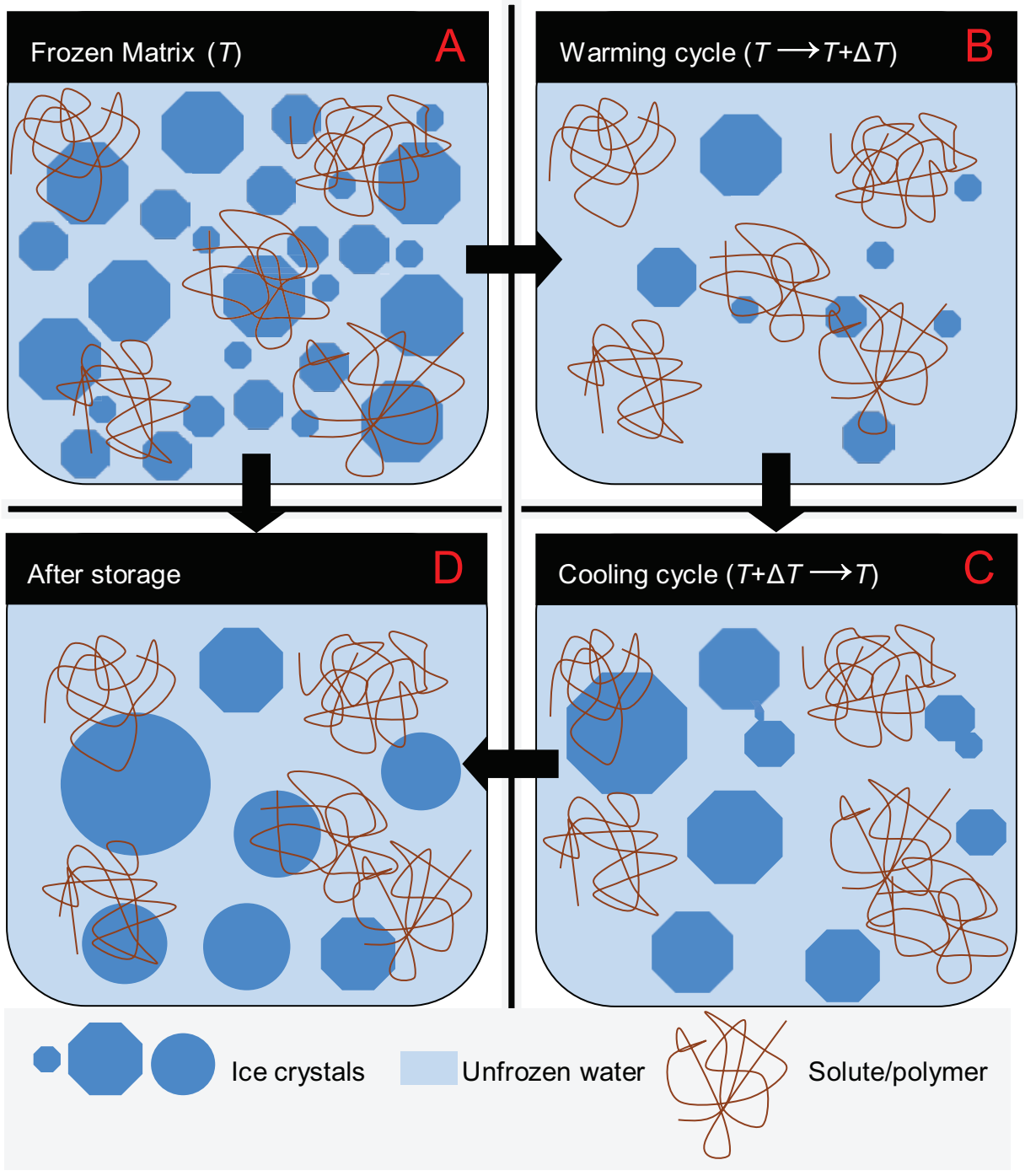
Frozen Matrix (T)
A
Warming cycle (T ⟶ T+ΔT)
B
After storage
D
Cooling cycle (T+ΔT ⟶ T)
C
Ice crystals
Unfrozen water
Solute/polymer

Figure 1

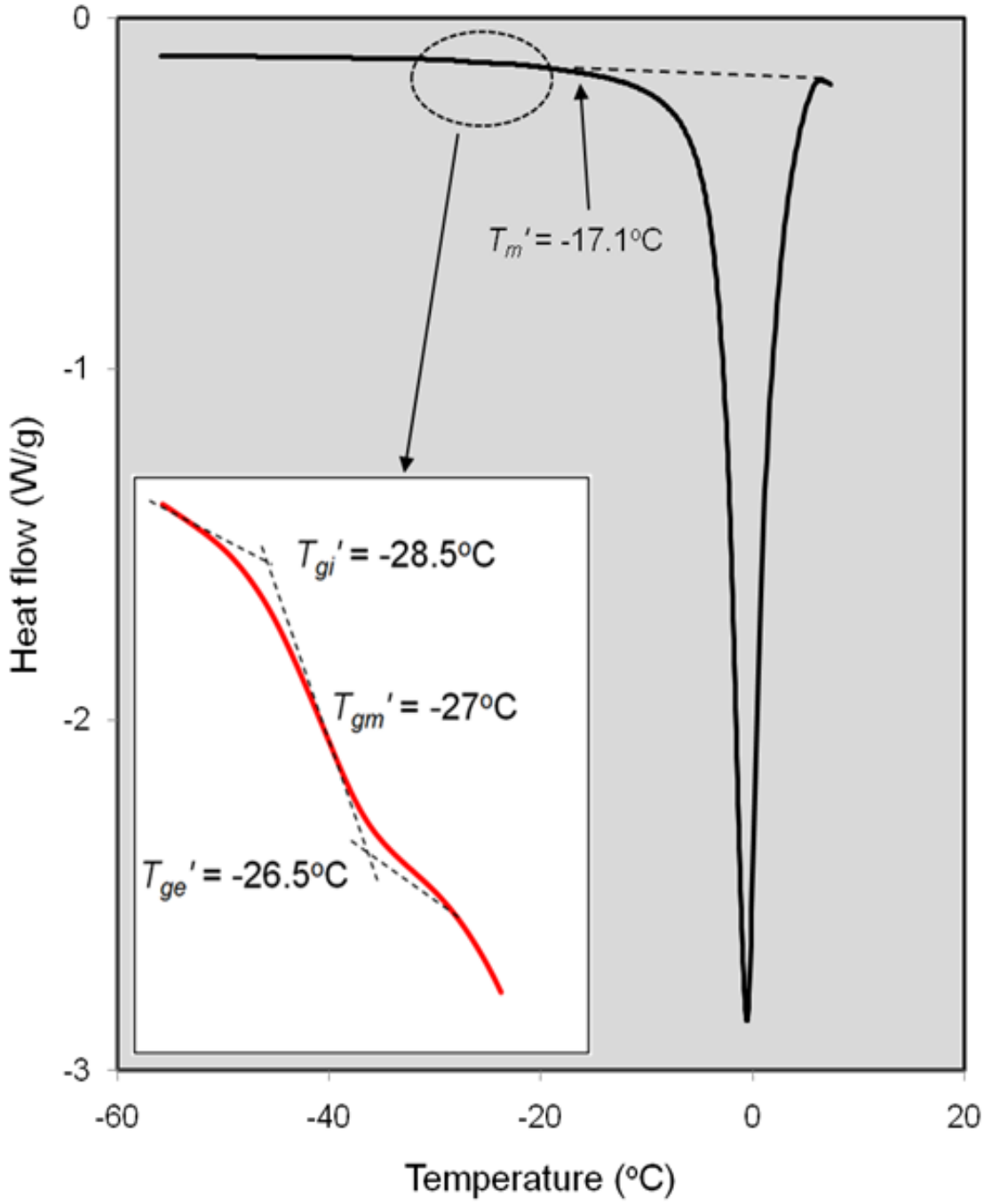
0
-1
-2
-3
Heat flow (W/g)
T_m' = -17.1°C
T_{gi}' = -28.5°C
T_{gm}' = -27°C
T_{ge}' = -26.5°C
-60
-40
-20
0
20
Temperature (°C)

Figure 2

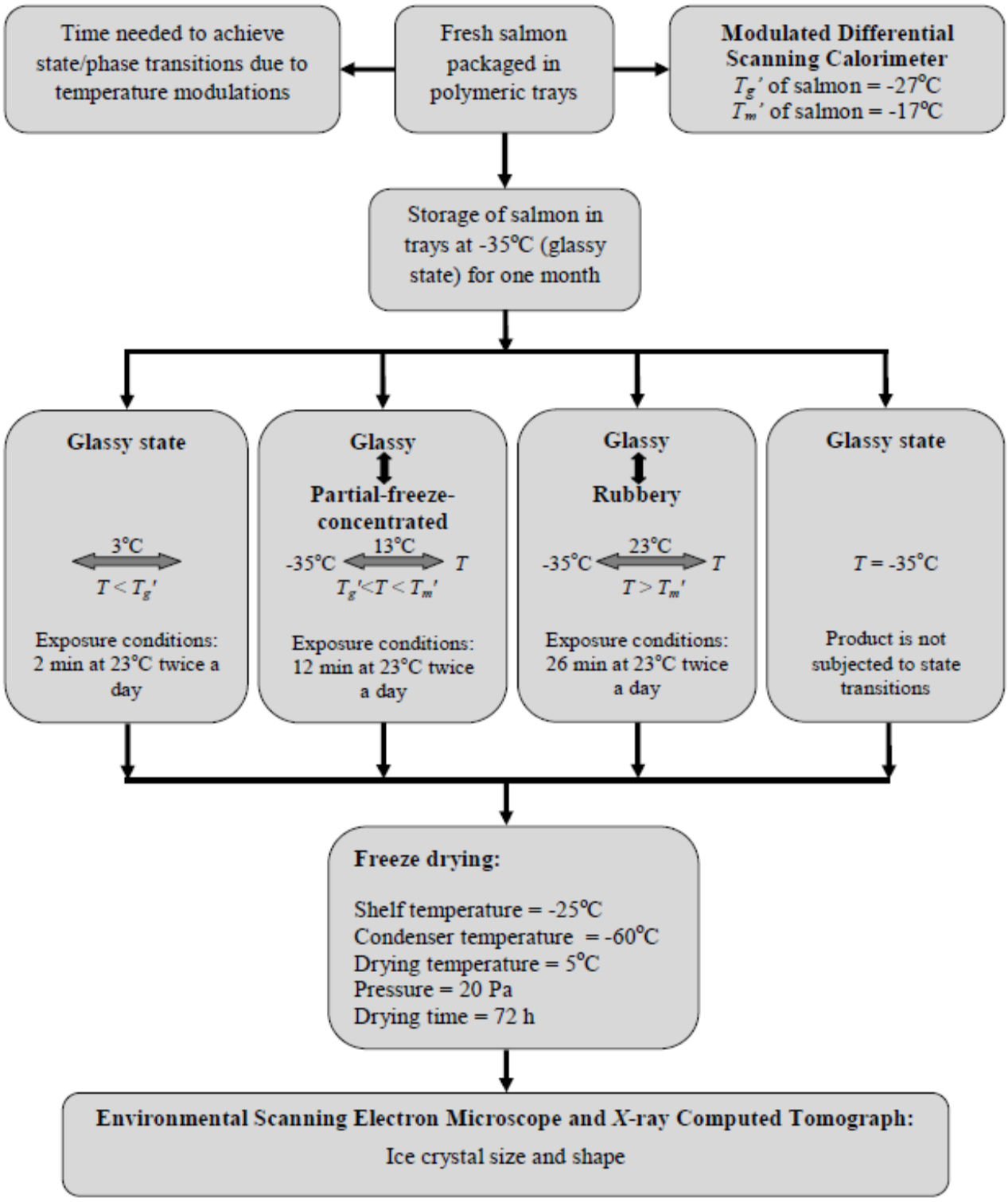
Time needed to achieve state/phase transitions due to temperature modulations
Fresh salmon packaged in polymeric trays
Modulated Differential Scanning Calorimeter
T_g' of salmon = -27°C
T_m' of salmon = -17°C
Storage of salmon in trays at -35°C (glassy state) for one month
Glassy state
3°C
$T < T_g'$
Exposure conditions: 2 min at 23°C twice a day
Glassy
Partial-freeze-concentrated
-35°C 13°C T
$T_g' < T < T_m'$
Exposure conditions: 12 min at 23°C twice a day
Glassy
Rubbery
-35°C 23°C T
$T > T_m'$
Exposure conditions: 26 min at 23°C twice a day
Glassy state
T = -35°C
Product is not subjected to state transitions
Freeze drying:
Shelf temperature = -25°C
Condenser temperature = -60°C
Drying temperature = 5°C
Pressure = 20 Pa
Drying time = 72 h
Environmental Scanning Electron Microscope and X-ray Computed Tomograph:
Ice crystal size and shape

Figure 3

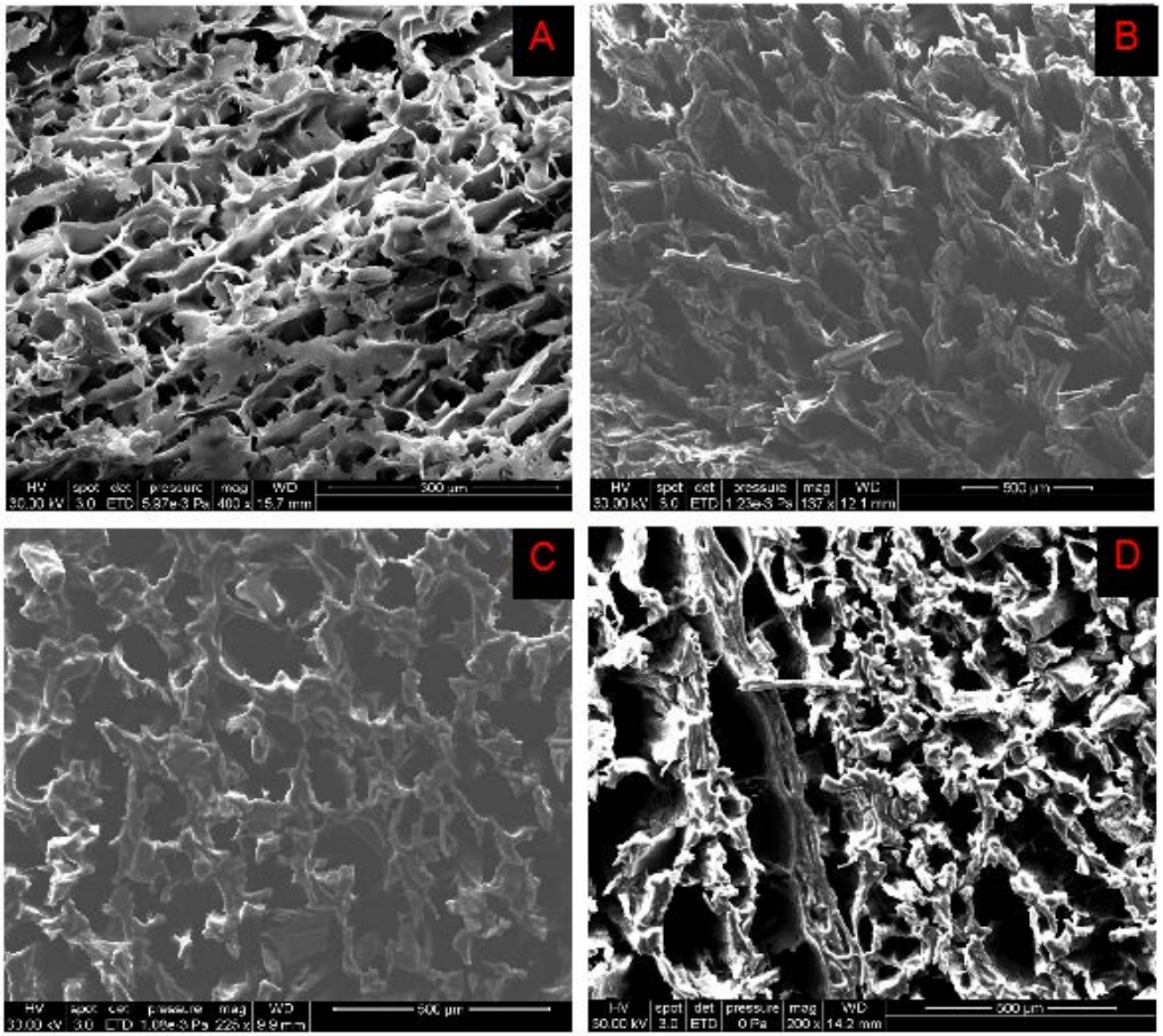

Figure 4

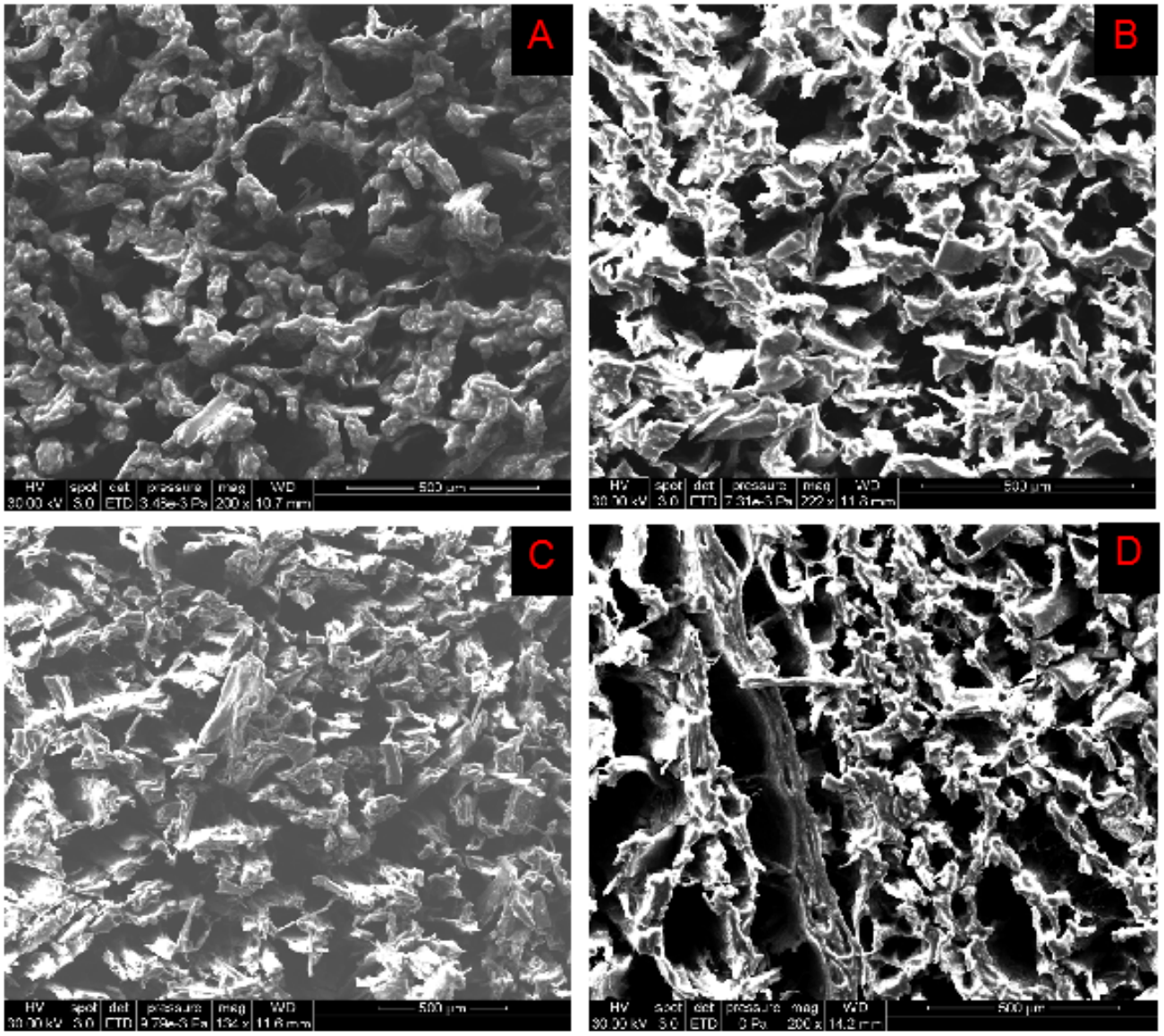

Figure 5

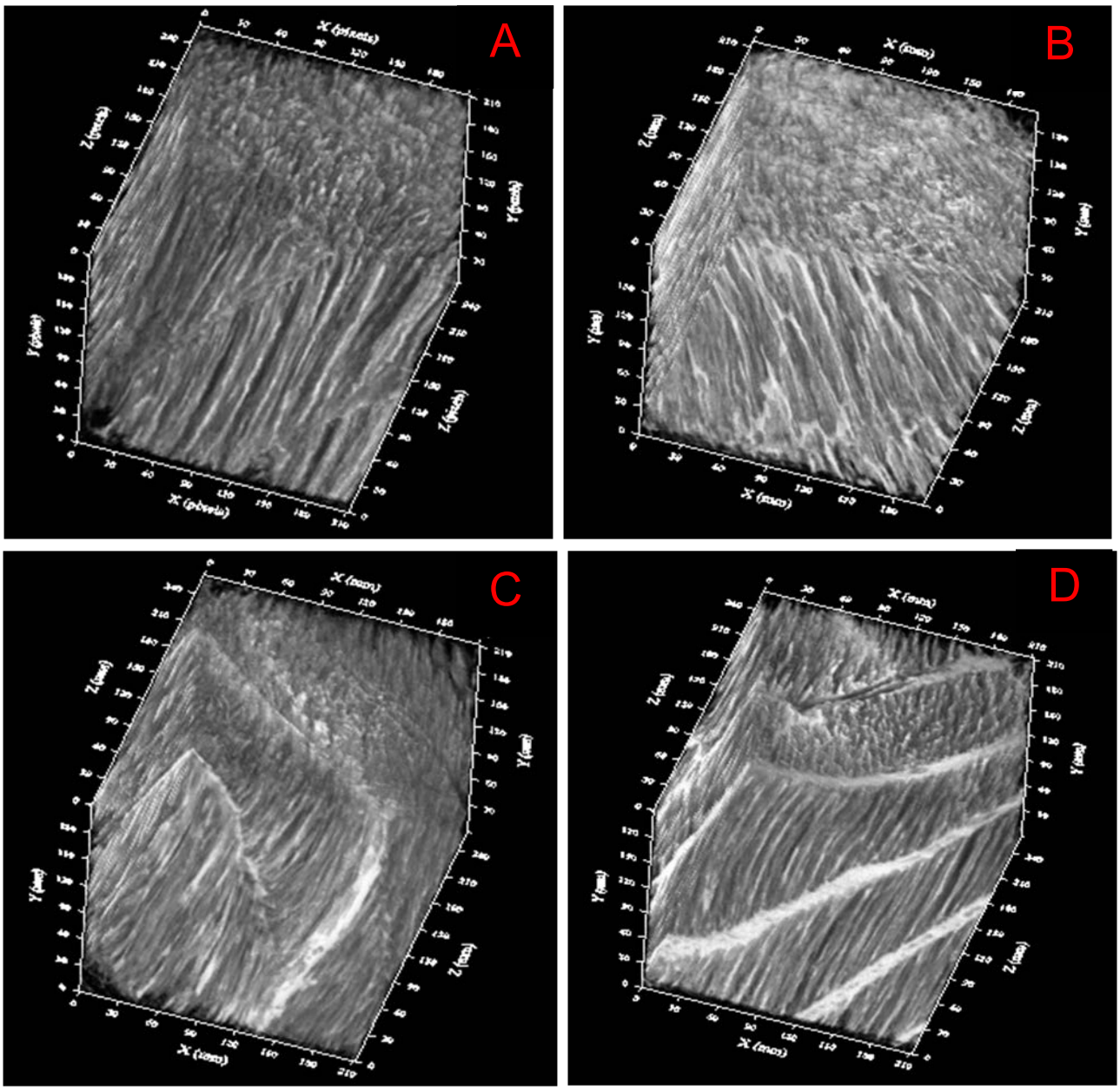

Figure 6

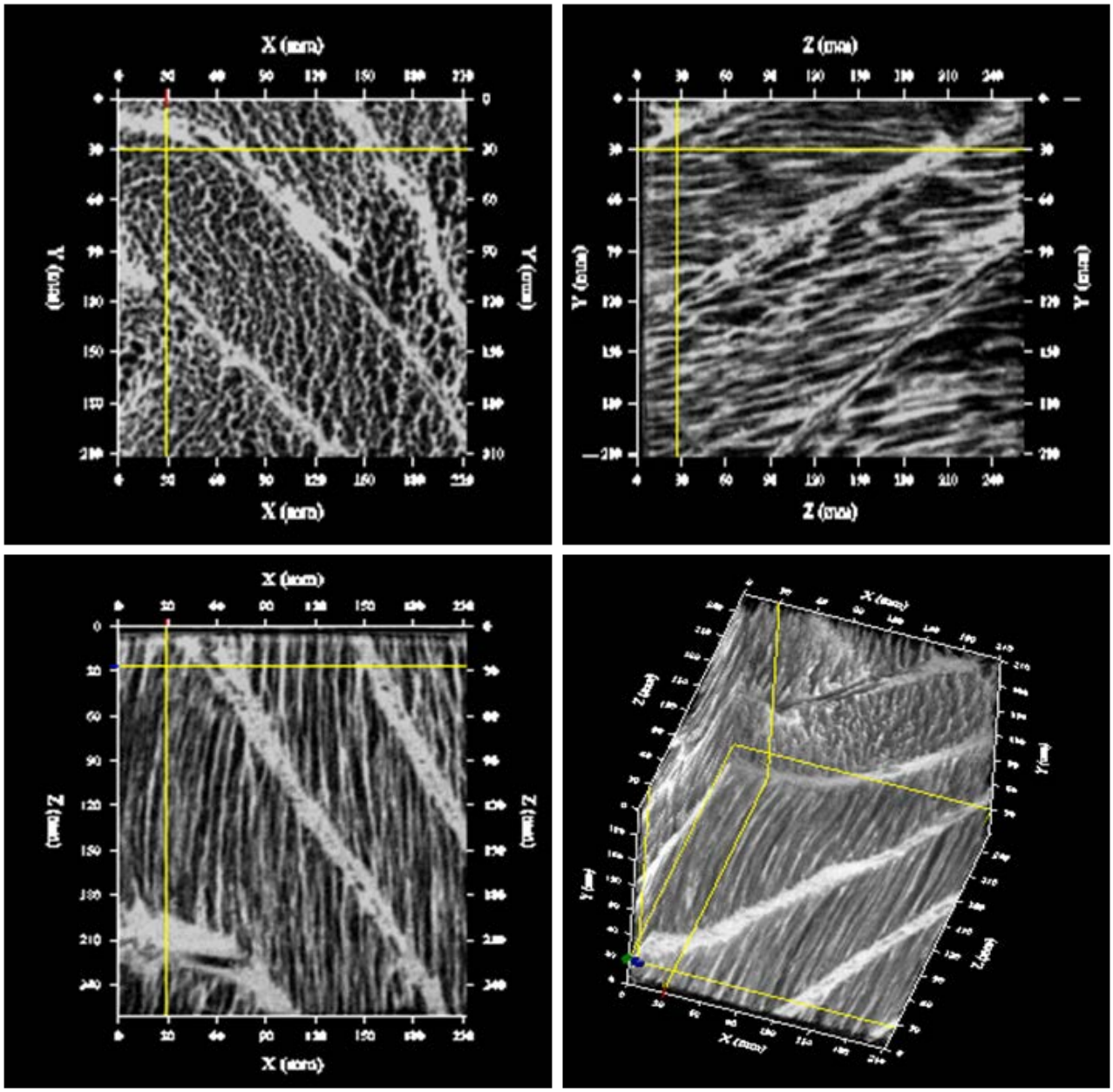

Figure 7

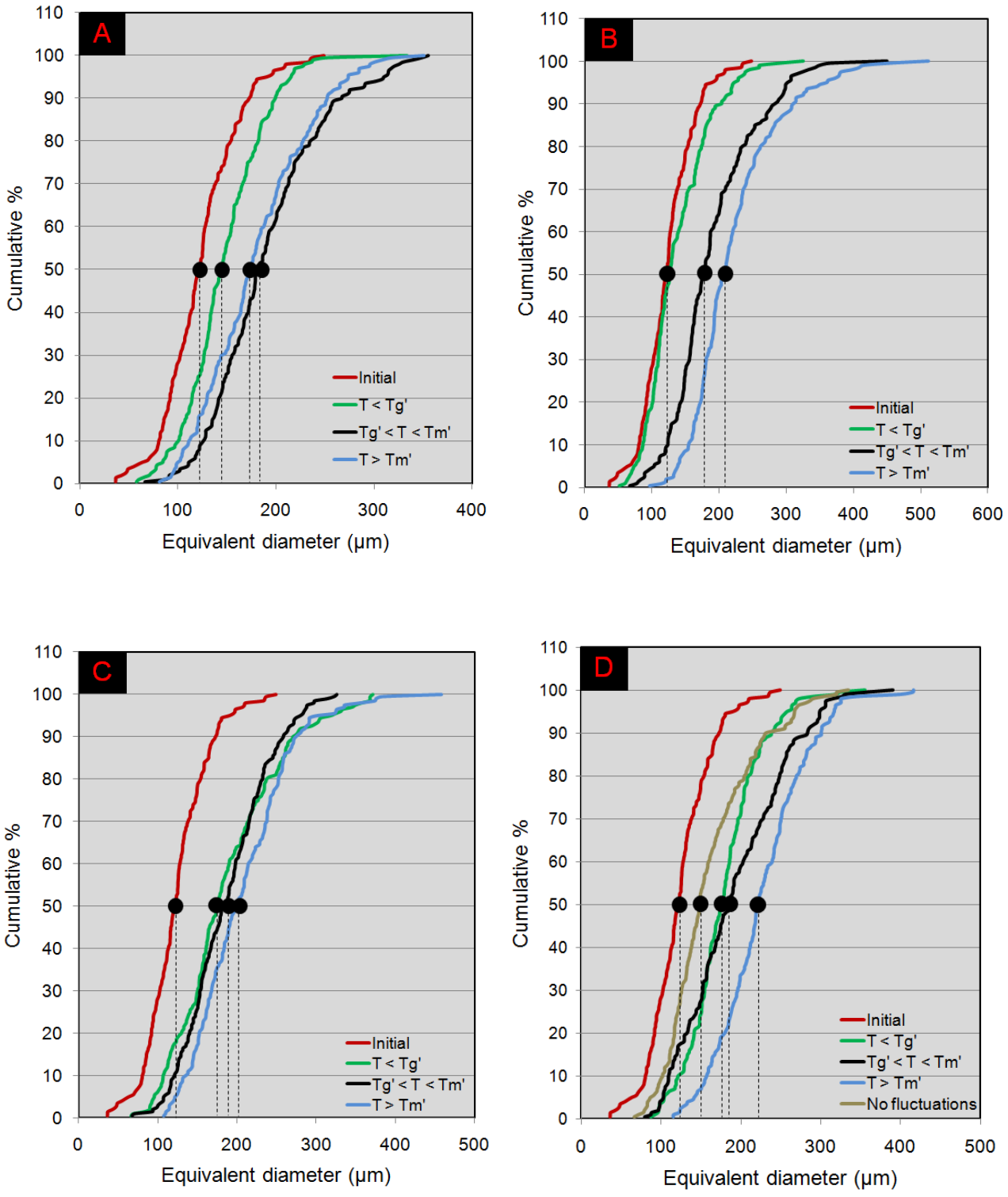
A
B
C
D
Cumulative %
Equivalent diameter (µm)
Initial
T < Tg'
Tg' < T < Tm'
T > Tm'
No fluctuations

Figure 8

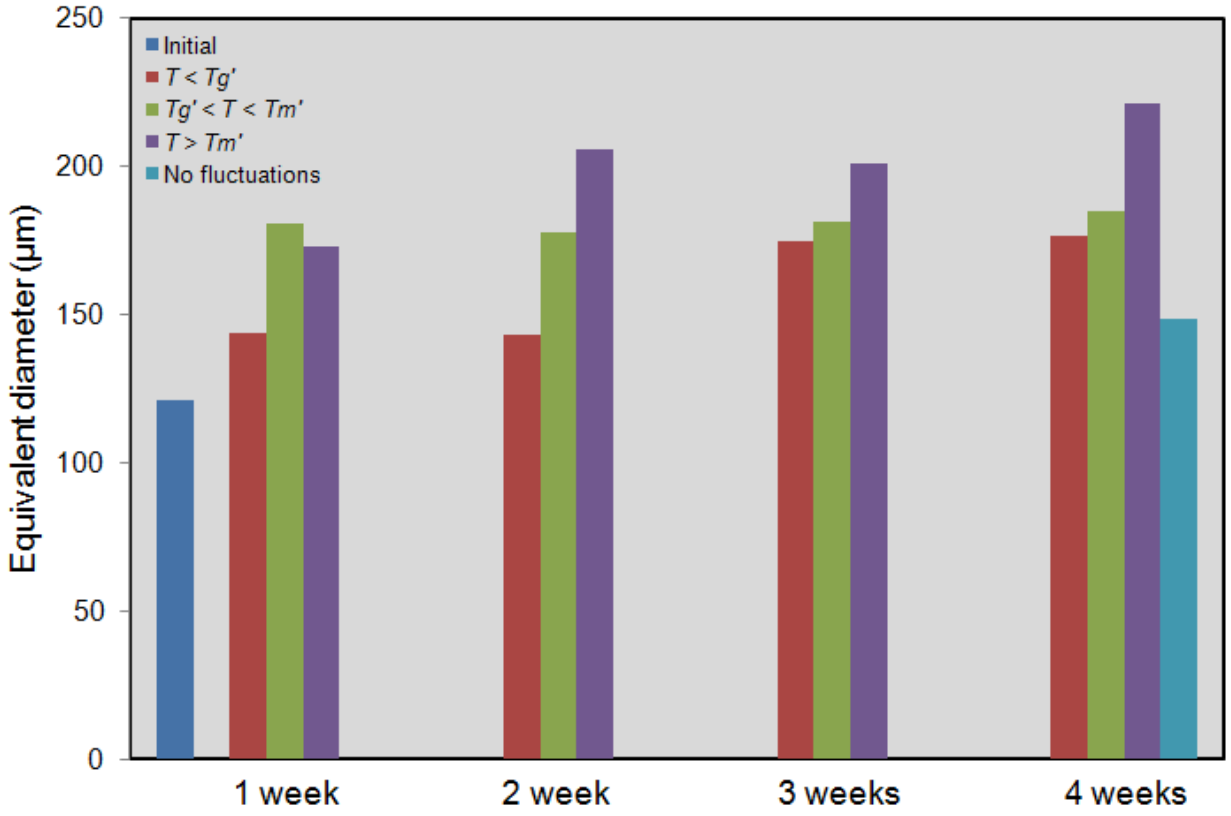
250
200
150
100
50
0
Equivalent diameter (µm)
Initial
T < Tg'
Tg' < T < Tm'
T > Tm'
No fluctuations
1 week
2 week
3 weeks
4 weeks

Figure 9

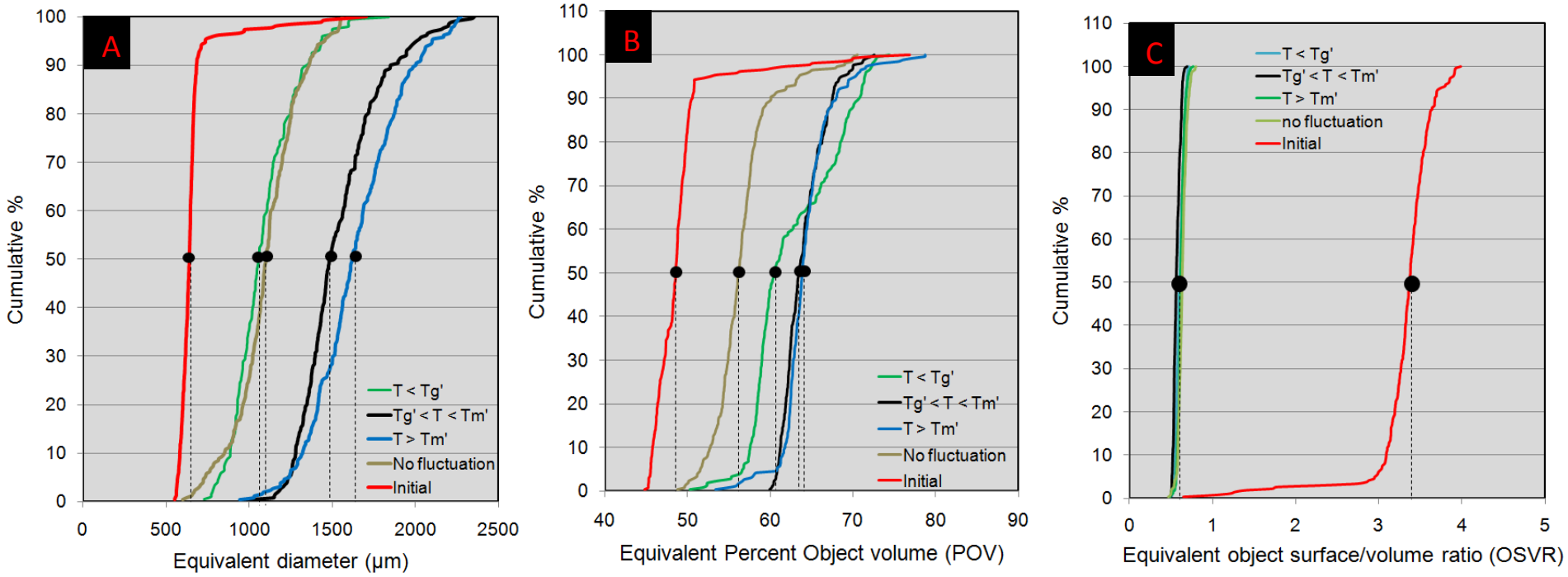
A
Cumulative %
Equivalent diameter (µm)
T < Tg'
Tg' < T < Tm'
T > Tm'
No fluctuation
Initial
B
Cumulative %
Equivalent Percent Object volume (POV)
T < Tg'
Tg' < T < Tm'
T > Tm'
No fluctuation
Initial
C
Cumulative %
Equivalent object surface/volume ratio (OSVR)
T < Tg'
Tg' < T < Tm'
T > Tm'
no fluctuation
Initial

Figure 10

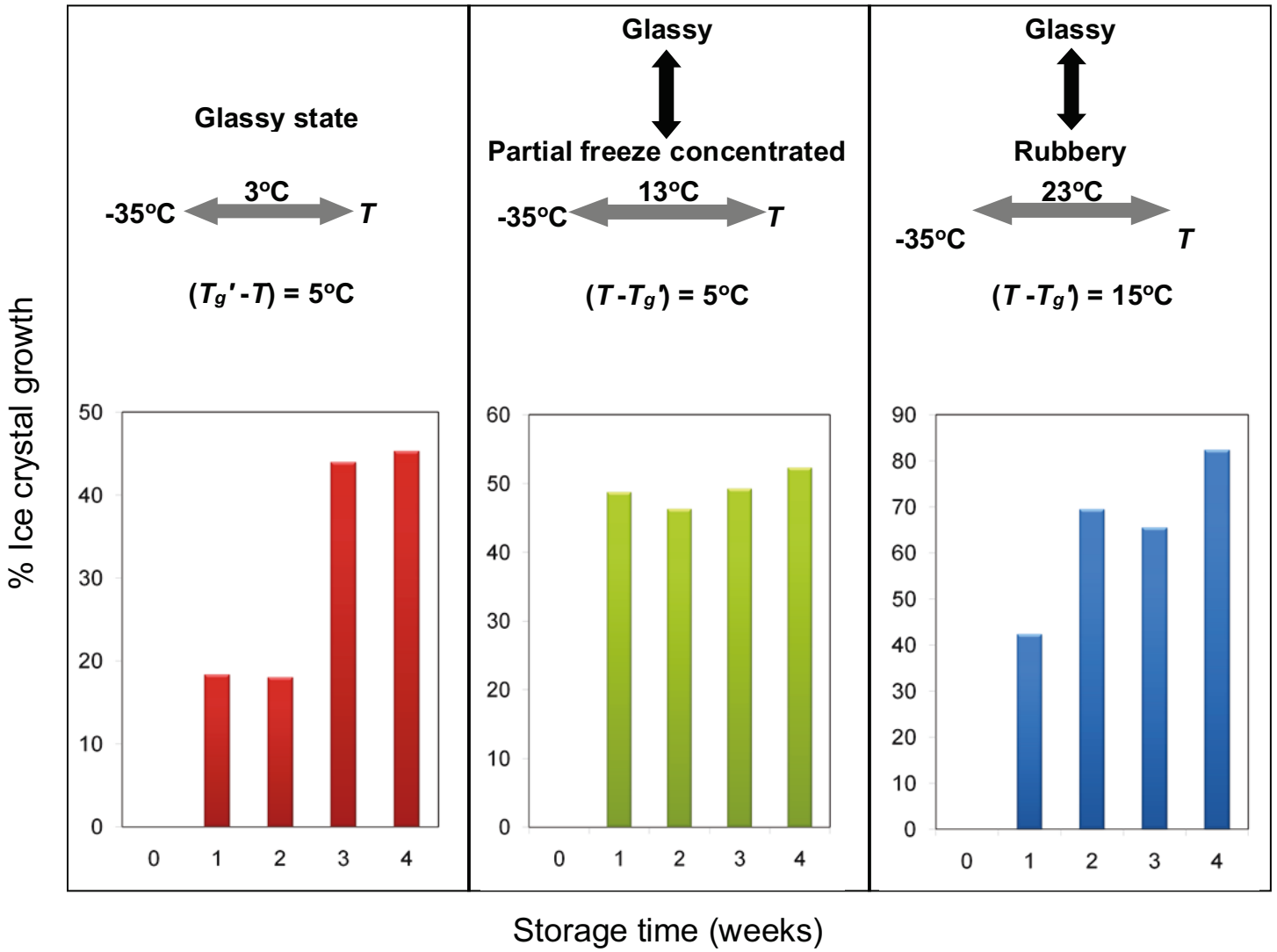
Glassy state
-35°C
3°C
T
(Tg' -T) = 5°C
Glassy
Partial freeze concentrated
-35°C
13°C
T
(T -Tg') = 5°C
Glassy
Rubbery
-35°C
23°C
T
(T -Tg') = 15°C
% Ice crystal growth
Storage time (weeks)
0
10
20
30
40
50
60
70
80
90
0 1 2 3 4

Figure 11

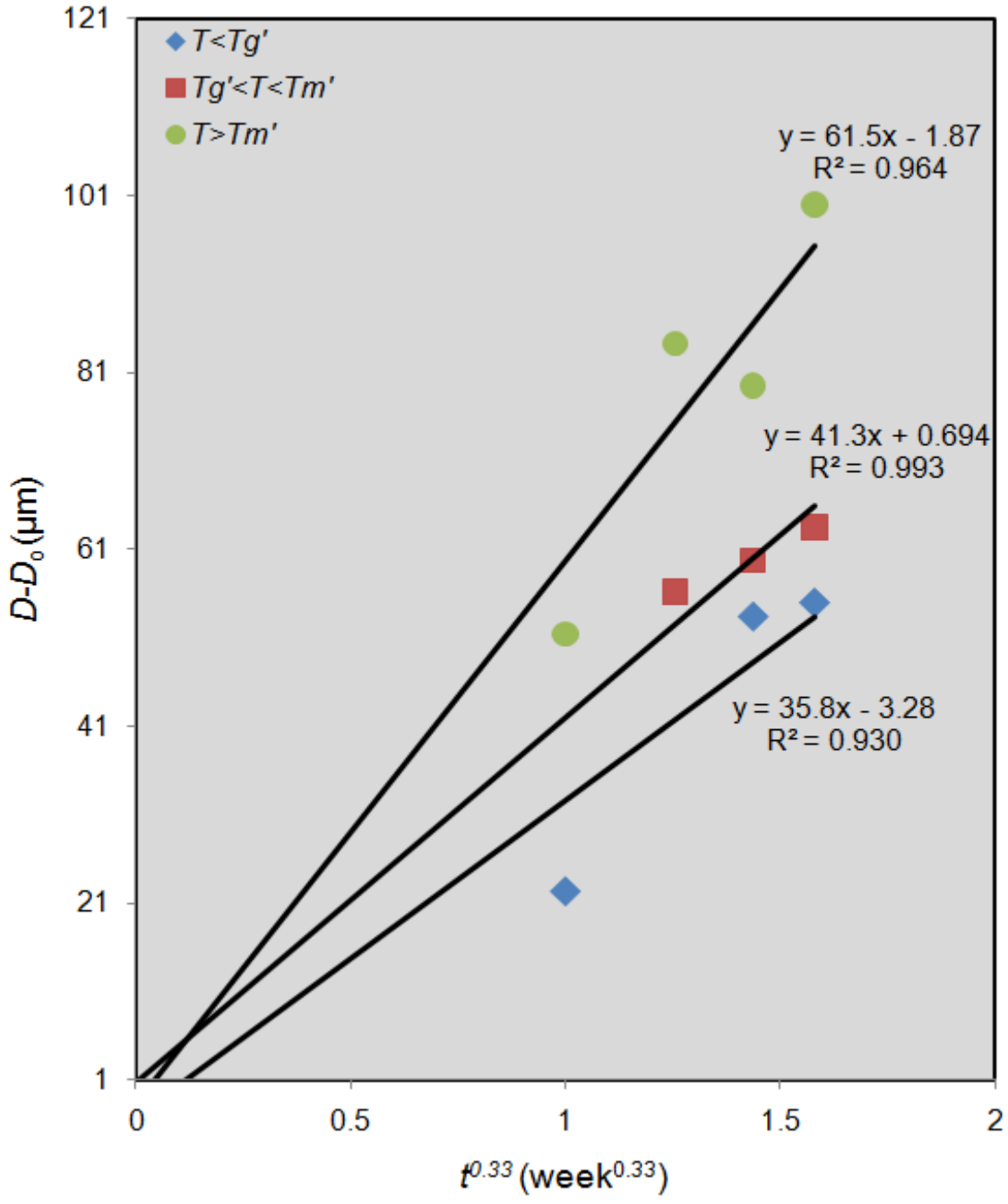
121
101
81
61
41
21
1
0
0.5
1
1.5
2
D-D0 (µm)
t0.33 (week0.33)
T<Tg'
Tg'<T<Tm'
T>Tm'
y = 61.5x - 1.87
R² = 0.964
y = 41.3x + 0.694
R² = 0.993
y = 35.8x - 3.28
R² = 0.930

Figure 12

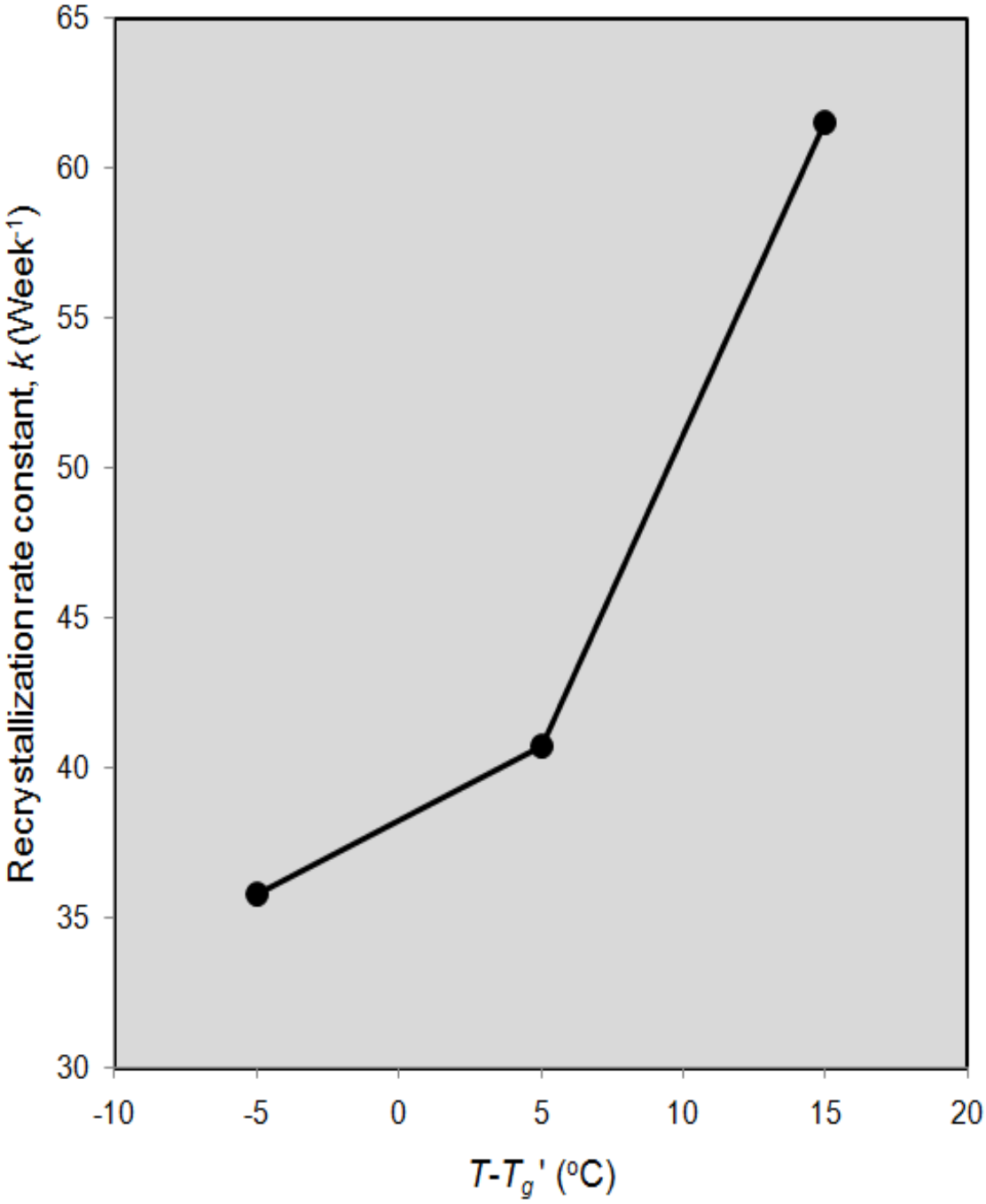
65
60
55
50
45
40
35
30
Recrystallization rate constant, k (Week-1)
-10
-5
0
5
10
15
20
T-Tg' (oC)

Figure 13